Article

Mott Law $\exp(T_0/T)^{1/4}$ and Scaling Properties of Oxygen Defect Tenorite $CuO_{0.75}$

[Danijel Djurek](#) [*] , [Mladen Prester](#) , Djuro Drobac , [Vilko Mandić](#) , [Damir Pajić](#)

Article

Mott Law $\exp(T_0/T)^{1/4}$ and Scaling Properties of Oxygen Defect Tenorite $CuO_{0.75}$

Danijel Djurek [1], Mladen Prester [2], Djuro Drobac [2], Vilko Mandić [3] and Damir Pajić [4]

[1] Alessandro Volta Applied Ceramics (AVAC), Augusta Šenoe 14, HR-49247 Zlatar Bistrica, Croatia

[2] Institute of Physics, Bijenička cesta 46, HR-10000 Zagreb, Croatia

[3] University of Zagreb Faculty of Chemical Engineering and Technology, Trg Marka Marulića 19, HR-10000 Zagreb, Croatia

[4] Department of Physics, Faculty of Science, University of Zagreb, Bijenička cesta 32, HR-10000 Zagreb, Croatia

* Correspondence: danijel@avac.hr

Abstract: The novel copper oxide $CuO_{0.75}$ has been prepared by slow oxidation of Cu_2O. The compound retains the original crystallographic structure of tenorite CuO, despite considerable presence of disordered oxygen vacancies. The $CuO_{0.75}$ resembles mixed valence oxide Cu^{2+}/Cu^{1+}, while the unit cell contains one oxygen vacancy. Performance-wise, the electric resistivity and magnetic susceptibility data follow the Anderson-Mott localization theories. Exponential localization decay rate was found to be α^{-1} = 2.1 nm, in line with modern scaling theories. Magnetic double exchange interaction, mediated by oxygen vacancies, results, by cooling, in Zener conductivity at $T \sim 122$ K, which is followed by antiferromagnetic transition at $T \sim 51$ K. The obtained results indicate, the $CuO_{0.75}$ compound can be perceived as showcase material for demonstration of new class of high performance paramagnetic materials.

Keywords: localization; scaling; oxygen defect tenorite; Mott $T^{-1/4}$ law; metal-insulator transition

1. Introduction

On the eve of localization theories in disordered systems Landauer [1] put forward the systematic calculation of the electric conductivity of metals containing point defects and derived an equation $\sigma = e^2/h \cdot [\Sigma T_i]$; summation is extended over scattering obstacles. Equation is widely used in semiconducting nanostructures, and pre-factor is named Landauer quantum conductance entering in various localization theories, quantum Hall effect, and symbolizes a way toward more universality in the solid state research.

The groundbreaking progress on localization in disordered systems, followed by Anderson [2] and Mott [3], triggered a further tremendous search for universality of magnetic and electric properties in solid state physics, optics, etc. The quantum mechanical functions in localized systems are confined in a finite region and they decay exponentially at higher distances. The localization phenomena cover various materials [4,5] and optics [6-8]. Experimental data, however, derived from the real objects are scarce and dominantly restricted to the resistive measurements [9,10], while accompanied magnetic effects, superposed to resistivity data are rare to trace in the scientific literature.

This paper aims to describe the preparation of the novel copper oxide $CuO_{0.75}$, indicated by disordered oxygen vacancies, while the X-ray diffraction data stress out maintaining the original structure of the tenorite CuO. In addition to the resistivity, $CuO_{0.75}$ displays an interesting set of magnetic effects, which start by cooling from $T \sim 122$ K and are followed by antiferromagnetic transition at $T \sim 51$ K. In the next step, the experimental data will be discussed in terms of Mott and Anderson theories, as well as, modern scaling models. However, difficulties arise from the fact that theories and models dominantly deal with metals, while $CuO_{0.75}$ is non-metal indicated by a huge dielectric permittivity $\varepsilon \sim 1.3 \cdot 10^3$, evaluated independently in these experiments.

2. Experimental

Oxygen defect form $CuO_{0.75}$ was produced from the powdered cuprous oxide Cu_2O of the particle size 0.5 microns and heated at 388 K in 4 bars oxygen atmosphere. Prior to reaction the powder was heated in vacuum at 423 K in order to remove the traces of gases: like moisture, CO_2 and SO_2. The slow reaction was monitored during 10 – 12 days by use of the pressure gauge and terminated when oxygen pressure was reduced to the value indicating the necessary stoichiometry $CuO_{0.75}$. The final product was raw and very hard cluster. Oxygen content was additionally verified by decomposition in 2 bar H_2 atmosphere at 673 K.

The powder obtained by subsequent reground of the raw cluster (R-sample) was pressed into pellets of 8 mm in diameter and d=0.9 mm thickness. In order to measure the four probes electric resistance, the 100 microns gold wires were pressed together with powder. Raw $CuO_{0.75}$ is an insulator, but it was observed that conductance may be induced by applied DC current starting with 1 μA and gradually increasing up to 1.5 mA during repeated annealing-cooling cycles (DC-samples) in argon atmosphere. Annealing temperature was 908 K, while the final conductivity of DC samples at room temperature (RT) saturated at $0.08–1.25\cdot10^{-2}\,\Omega^{-1}m^{-1}$. It may be a tedious work to explain this interesting phenomenon in terms conventional chemical and metallurgical methodology. More recent findings [11,12] may provide some introductory ideas and hints on possible stimulation of disorder and corresponding increase of the conductivity by use of the conducting currents.

3. Results

Copper oxide CuO is narrow band p-type semiconductor and crystallographic unit cell belongs to the monoclinic group C2/c with cell dimensions $a = 0.4683$ nm, $b = 0.3421$ nm, $c = 0.5129$ nm; $\alpha = 90°$, $\beta = 90°$, $\gamma = 99.784°$. Unit cell contains 4 units formulas, and density is $\rho = 5.94$ g·cm^{-3}, while the oxygen defect form $CuO_{0.75}$ exhibits $\rho = 5.64$ g·cm^{-3}. Due to one oxygen vacancy per unit cell, $CuO_{0.75}$ is expected to be a mixed valence oxide with equal number of Cu^{2+} and Cu^+ cations. In this respect, $CuO_{0.75}$ resembles the copper oxide Cu_4O_3, known as paramelaconite, with the structure indicating CuO_2 chains along c-axis [13]. Pinsard-Gaudart and co-workers reported [14] the antiferromagnetic transition in Cu_4O_3 at 42 K. XRD data of $CuO_{0.75}$ are shown in Figure 1.
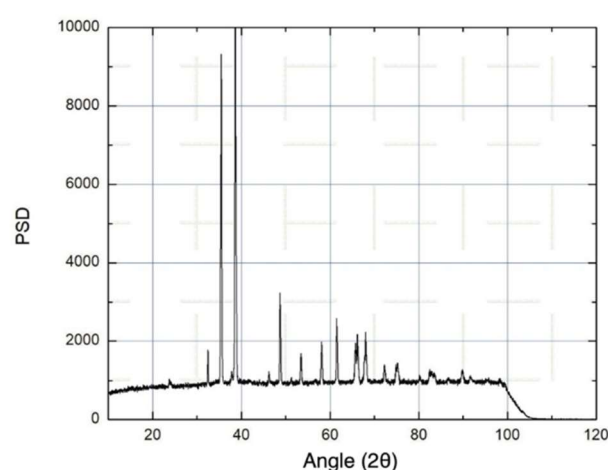
Figure 1. X-ray diffraction analysis of the copper oxide sample.

High resolution measurements of AC susceptibility were performed on R- and DC-samples by use of Cryobind susceptometer, and real and imaginary parts are shown in Figure 2. Samples exhibit a surprising temperature dependence of the susceptibility, and several effects are included. By heating to RT, the magnetic susceptibility reveals three features. At $T = 51$ K, both DC- and R-samples,

undergo an antiferromagnetic transition. The next feature appears in DC sample at $T = 101$ K, while at $T_C = 122$ K, DC-sample resembles the paramagnetic transition. Both cited transitions are absent in the raw R-sample. At $T > 122$ K DC sample obeys the Stoner expression $\chi = \chi_P / [1 - U \cdot N(E_F)]$, while the quantities χ_P, U and $N(E_F)$ are in the respective order; Pauli susceptibility, Coulomb repulsion energy U(Joule·m³) and density of states (DOS) on the Fermi surface. The Pauli susceptibility χ_P and DOS were evaluated from the inverse susceptibility $1/\chi$ plotted versus $1/T$. Horizontal dashed line reflects a contribution of the Pauli susceptibility and foreign ingredients; the latter must be subtracted, after an independent measurement on non-reacted Cu_2O. Dimensionless Pauli susceptibility is $\chi_P = 2.9 \cdot 10^{-6}$, while DOS was calculated [15] from $\chi_P = \mu_0 \cdot \mu_B^2 \cdot N(E_F)$, giving $N(E_F) = 2.8 \cdot 10^{46}$ Joule⁻¹·m⁻³. The Fermi energy E_F was separately derived from number of states $n = 1/V_0 = 2.4 \cdot 10^{28}$ m⁻³, and V_0 means the volume of the crystallographic unit cell. Fermi wave number is given as $k_F = (3\pi^2 \cdot n)^{1/3}$, and $E_F = 3.3$ eV.
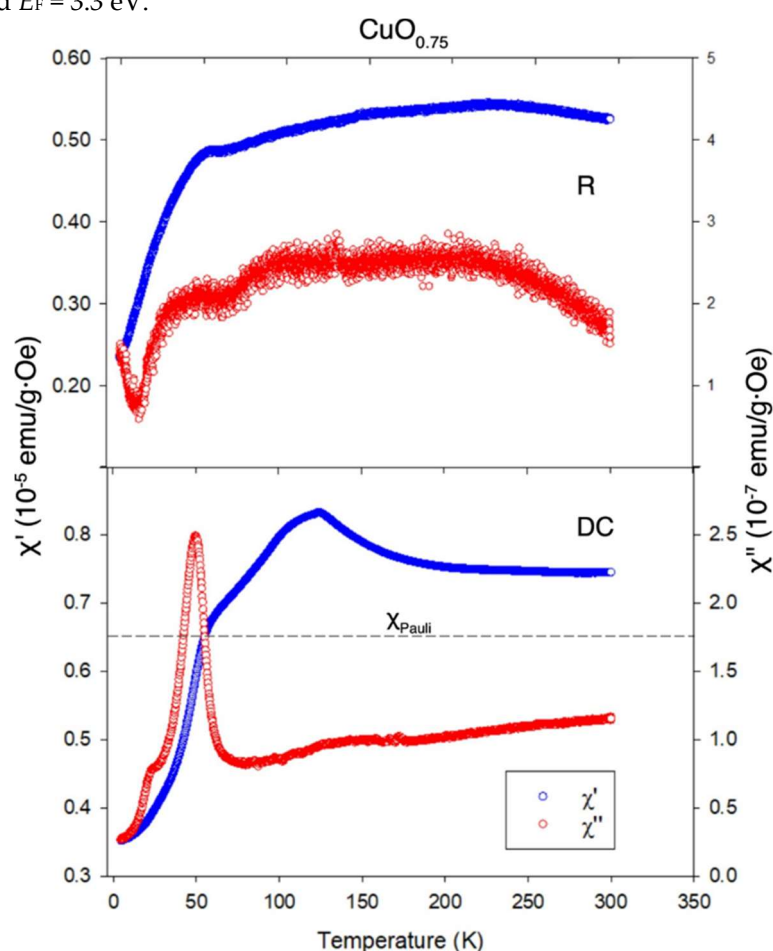

Figure 2. Temperature dependence of the real and imaginary parts of AC magnetic susceptibility of $CuO_{0.75}$ recorded by a compensated secondary coils susceptometer at 231 Hz and 1.26 Oe (zero-peak): (a) pellet prepared from the raw powder and multiply annealed at 908 K in 0.5 bar argon gas.(b) pellet multiply annealed in 0.5 bar argon gas at 908 K under passing DC current started at 10^{-6} A, and finished at $1.5 \cdot 10^{-3}$ A. Heating rate was 430 K/ hour⁻¹, annealing lasted 0.5 hour, and cooling was in 8.8 hours by normal cooling rate of the oven. The sample is the same as used in the presented resistance measurement.

Figure 3 presents the resistance of DC-sample measured by cooling and heating in the range 415 – 80 K. It is evident the linear dependence of ln$R$ on $T^{-1/4}$ down to $T_C = 122$ K, when strong linear increase converts in stagnation, which is followed by the sharp downturn at $T = 101$ K. Linear dependence of ln$R$ on $T^{-1/4}$ is the characteristic behavior of the disordered 3 dimensional (3D) system indicated by localization of the electronic states. Anderson put forward that, in disordered systems, diffusion theories of the conductivity must be replaced by models based upon quantum jumps

between the localized states. Continuing upon such a course, Mott developed theory[17] of the variable range hopping, and logarithm of the resistivity was derived as

$$ln\rho = 2\alpha R + 1/(4\alpha\pi/3)k_B T R^3 N(E_F) \qquad R = [\alpha k_B T N(E_F)]^{-1/4} \quad (1)$$

where $1/\alpha$ and R are localization length and hopping range respectively. This expression was fitted to the measured dependence $\ln R$ on $T^{-1/4}$ in the temperature interval 122 – 415 K when metallic state sets up by further heating. An evaluation of the localization length gives $\alpha^{-1} = 2.1 \cdot 10^{-9}$ m, while the variable range length at $T = 122$ K is $R = 2.3 \cdot 10^{-9}$ m. R decreases slowly by heating, and Mott expression of the level spacing between two states reads $\Delta = \alpha^3/N(E_F) \sim 18.8$ meV.
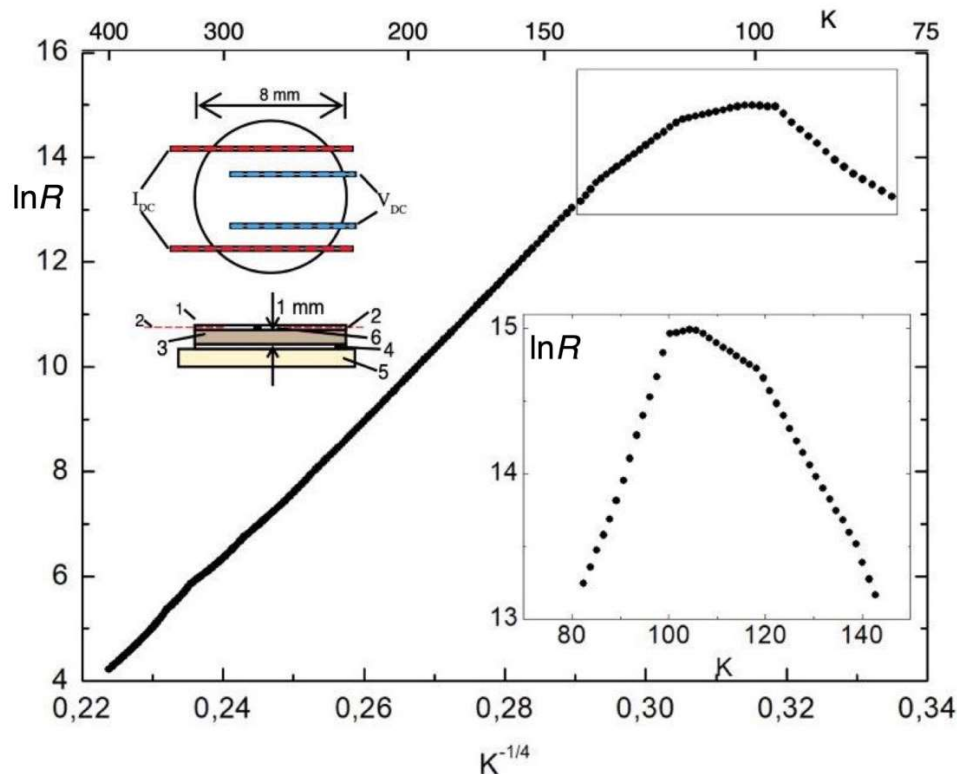
Figure 3. DC electric resistance of the annealed DC-sample CuO$_{0.75}$. In-pressed gold wires, 100 microns in diameter, provide four probe measurements. In order to eliminate the contribution of thermopower, cooling-heating cycle was proceeded slowly and extended up to 44 days. Liquid nitrogen level in the surrounding cooling bath was maintained constant, while evaporation was compensated by introduction of the fresh liquid nitrogen by drop-and-drop method via special pump. Copper-constantan thermocouple, consisting of 50 microns wires was attached to the pellet by temperature resistant lacquer, and enforced by the silk weave, as it is shown in the inset. Thermocouple was separated from the pellet by 30 microns mica foil. It is evident the logarithmic plot of the resistance versus $T^{-1/4}$ in the range 122 – 415 K. Inset shows temperature dependence of the logarithm of the resistance in the range 88 – 140 K.

Measured electric conductance of CuO$_{0.75}$ at $T = 415$ K was $G_0 = 1.5 \cdot 10^{-2} \Omega^{-1}$, and evaluated conductivity is $\sigma_0 = 0.17 \ \Omega^{-1} \cdot cm^{-1}$. When this value should be compared to Mott minimum *metallic* conductivity $\sigma_{min} = \pi^2 \cdot e^2/8 \cdot z \cdot h \cdot c$ [ref.16, p.31], it must be encountered the dielectric permittivity of CuO$_{0.75}$, $\varepsilon = 1.3 \cdot 10^3$ in the temperature interval 100 – 415 K. The renormalized value reads $\sigma = \varepsilon \cdot \sigma_0 \sim 221 \ \Omega^{-1} cm^{-1}$, and it is comparable to the Mott value $\sigma_{min} = 300 \ \Omega^{-1} \cdot cm^{-1}$. In further calculations we replace lattice parameter c by α^{-1} distant localized scatters.

The measurements of hysteresis performed by use of SQUID, are presented in Figure 4. Measurements of magnetization, dependent on magnetic field at various stable temperatures, sound for antiferromagnetic state below 50 K. Bending of hysteresis around small fields could originate from

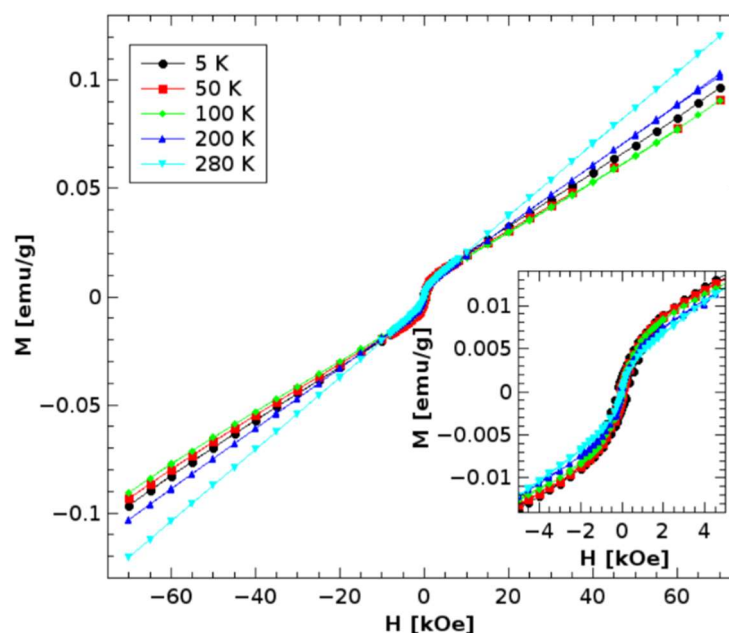superparamagnetism of nano-clusters, which may reflect the localized states bound to distinct regions.

Figure 4. The SQUID data evaluated in DC-sample $CuO_{0.75}$.

4. Discussion

Pinsard-Gaudart and co-workers calculated in paramelaconite Cu_4O_3 the magnetic double-exchange interaction E = 48,3 K between nearest neighbor Cu^{2+} cations Cu^{2+}–O–Cu^{2+} (NN). Such a mechanism may also be certain in $CuO_{0.75}$, with oxygen vacancies involved in double-exchange Cu^{2+}–V_O–Cu^{2+} or Cu^{2+}–V_O–Cu^+. In support, Gao and co-workers [17] reported a weak ferromagnetism mediated by oxygen vacancies in CuO nanoparticles.

Downturn of the resistance in $CuO_{0.75}$ below 122 K may be explained by Zener model of the magnetic double exchange conductivity. Model was originally applied to the resistance [18] properties of strontium doped manganite $(La_{1-x}Sr_x)MnO_3$. An exchange is favored by the polarization of the hopping electrons between aligned cation spins Mn^{4+}–O–Mn^{3+}, which, in turn, enhances the electric conductance and the magnetization due to the itinerant electron contribution. Zener evaluated the electric conductance $G_Z = x \cdot e^2 E / h \cdot k_B T$. E and x are exchange energy and fraction of ions involved in the exchange respectively. G_Z may compete the resistance divergence $T^{-1/4}$ in $CuO_{0.75}$ at $T < 122$ K giving rise to a possible two fluid conductance. Calculated Zener conductivity reads $\sigma_Z \sim 380$ $\Omega^{-1} \cdot cm^{-1}$, while relative dielectric permittivity is absent in the evaluation.

Thouless [19] introduced dimensionless conductance $g = G \cdot h / e^2$. However, the ratio of the measured and Landauer conductance is impractical for testing the scaling theories by experiment, since measured conductance G is dependent on the sample thickness d, as being no uniquely defined parameter. We introduce dimensionless conductivity $g = \varepsilon \cdot \alpha^{-1} \cdot G \cdot h / d \cdot e^2$, and g gives Thouless energy $E_T = g \cdot \Delta$. Δ = 18.8 meV is the, above evaluated, level spacing, and from the resistance at T =415 K, Thouless energy reads E_T = 9.8 meV giving T_C=132 K, which should be compared to transition temperature T = 122 K. Thouless energy and corresponding temperature mark the melting of the localized to extended states, while, upon heating, the $T^{-1/4}$ regime starts at temperature T= 122 K, and extends up to 415 K.

In the next step, an attempt is presented to compare the resistance data to scaling model put forward by Abrahams and co-workers (AALR) [20]. The problem arises to define the universal scaling length L based on given experimental data. The choice proposed by AALR is the mean free path l, although l is doubtful because of strong dependence on temperature. Following a search for common points of AALR model, Mott theory and our experimental data, we introduce localization decay L=α^-

[1] as a scaling length, since it is independent of temperature. AALR theory introduces parameter $\beta = d(\ln g)/d(\ln L)$ indicating $\beta = 0$ at the metal-insulator transition. The comparatively easy calculation, for the case $CuO_{0.75}$, starts with an elimination of the temperature in Equation (1), which gives the dimensionless conductivity $g = (\varepsilon \cdot \alpha^1 \cdot h \cdot \sigma_0/e^2) \cdot \exp{-\alpha R[2 + \frac{3}{4}\pi]}$. This expression matches the AALR result for 3D system, and little more algebra results in $\beta = \ln g$, giving $\beta = 0$ for $g = 1$, means that metal-insulator transition may be expected when the renormalized conductivity $\varepsilon \cdot \alpha_0$ approaches the Landauer quantum conductivity $e^2 \cdot \alpha/h$ proceeded between two localized points distant α^1. In the case $CuO_{0.75}$ this happens at $T \sim 415$ K, when $\exp(T_0/T)^{1/4}$ regime starts by cooling.

5. Conclusions

In conclusion, a novel copper oxide $CuO_{0.75}$ was prepared. It is indicated by one oxygen vacancy per unit cell and exhibits the crystallographic structure of a tenorite CuO. In the interval 122 – 415 K, electric resistance is temperature dependent according to the Mott law $\exp[(T_0/T)^{1/4}]$. Anderson theory of localization and Mott theory of variable hopping were successfully applied, and characteristic length of exponential decay of the localized state was evaluated $\alpha^{-1} = 2.1$ nm, while variable hopping range is $R = 2.3 \cdot 10^{-9}$ m at $T = 122$ K. It has been shown that Mott's concept of minimum conductivity in metals σ_{min} may be extended to nonmetal $CuO_{0.75}$, giving rise to a possible universal physical constant. In addition, σ_{min} has been evaluated by taking in account a calculated [21] ratio of critical localization potential and band width $V_{crit}/B = 2$, confirming this result as to be correct. Dimensionless Thouless conductivity g was calculated and corresponding Thouless energy E_T, converted to temperature, gives $T \sim 142$ K. In order to apply scaling theory of Abrahams and co-workers (AALR), $L = \alpha^{-1}$ is chosen as a scaling length, while β function reads $\beta = \ln g$. At $T = 122$ K magnetic measurements reveal the transition to a double exchange interaction indicated by Zener conductivity, which is comparable to the Mott conductivity σ_{min}. $CuO_{0.75}$ undergoes an antiferromagnetic transition at 51 K.

References

1. Landauer, R. Spatial Variation of Currents and Fields Due to Localized Scatters in Metallic conduction. *IBM Journal of Research and development*, **1** (3), 223-231 (1957).

2. Anderson, P,W. Absence of Diffusion in Certain Random Lattices. *Phys. Rev.* **109**,1492-1505 (1958).

3. Mott, N, F. Conduction in non-crystalline systems, *Phil. Mag.* **19**, 835-852 (1969).

4. Hu, H.A. et al. Localization of ultrasound in a three-dimensional elastic network. *Nat. Phys.* **4**, 945-948 (2008).

5. Chabanov, A.A.et al. Statistical signatures of photon localization, *Nature*. **404**, 850-853 (2000).

6. John, S. Electromagnetic Absorption in a Disordered Medium near a Photon Mobility Edge, *Phys. Rev. Lett.* **53**, 2169-2174 (1984).

7. Wiersma, D.S.et al. Localization of light in a disordered medium, *Nature*. **390**, 671-673 (1997).

8. Bücker,W. Preparation and dc conductivity of an amorphous organic semiconducting system, *Journal of Non-Crystalline Solids.* **12,**115-128 (1973).

9. Allen, F, R. & Adkins, C. J. Electrical Conduction in Heavily Doped Germanium, *Phil.Mag.* **26**, 1027-1042 (1972).

10. Norwood, T.E. & Fry, J.L. Energy Bands of VO. *Phys. Rev.* **B2**, 472-485 (1970).

11. Vojta, Th. et al. Infinite-randomness quantum critical point induced by dissipation. *Phys.Rev.* **B79**, 024401 (2009).

12. Chávez, Nahum C. et al. Disorder-Enhanced and Disorder-Independent Transport with Long-Range Hopping: Application to Molecular Chains in Optical Cavities. *Phys. Rev. Lett.* **126**,153201 (2021).

13. O'Keeffe, M. & Bovin, J.-O. The crystal structure of paramelaconite Cu_4O_3. *Am. Mineral.* **63**,180-185 (1978).

14. Pinsard-Gaudart, L. et al. Magnetic properties of paramelaconite (Cu_4O_3): A pyrochlore lattice with $S = \frac{1}{2}$, *Phys. Rev.* **B 69**, 104408, 1-9 (2004).

15. Aschcroft, N.W. & Mermin, N.D. Solid State Physics, Harcourt College Publisher, p. 663.(1976).

16.   Sir Nevill Mott. Metal-Insulator Transitions, Taylor & Francis, London. p.36 (1974).

17.   Gao, D. et al. Vacancy-Mediated Magnetism in Pure Copper Oxide Nanoparticles. *Nanoscale Res. Lett.* **5**, 769-772 (2010).

18.   Zener, C. Interaction between the *d*-Shells in the Transition Metals. II. Ferromagnetic Compounds of Manganese with Perovskite Structure. *Phas.Rev.***82** (3), 403-405 (1951).

19.   Thouless, D.J. Electrons in Disordered Systems and the Theory of Localization. *Physics Reports.***13**(3),93-142 (1974).

20.   Abrahams, E. et al. Scaling Theory of Localization: Absence of Quantum Diffusion in Two Dimensions. *Phys.Rev. Lett.* **42**(10), 673-676 (1979).

21.   Edwards, J.T. & Thouless, D.J. Numerical studies of localization in disordered systems, *J. Phys. C: Solid State Phys.* **5**, 807-2022 (1972).